

Vulnerability of Transport through Evolving Spatial Networks

Ali Molavi,¹ Hossein Hamzhepour,¹ and Reza Shaebani²

¹*Department of Physics, K.N. Toosi University of Technology, Tehran 15875-4416, Iran*

²*Department of Theoretical Physics and Center for Biophysics,
Saarland University, 66123 Saarbrücken, Germany*

Insight into the blockage vulnerability of evolving spatial networks is important for understanding transport resilience, robustness, and failure of a broad class of real-world structures such as porous media and utility, urban traffic, and infrastructure networks. By exhaustive search for central transport hubs on porous lattice structures, we recursively determine and block the emerging main hub until the evolving network reaches the impenetrability limit. We find that the blockage backbone is a self-similar path with a fractal dimension which is distinctly smaller than that of the universality class of optimal path crack models. The number of blocking steps versus the rescaled initial occupation fraction collapses onto a master curve for different network sizes, allowing for the prediction of the onset of impenetrability. The shortest-path length distribution broadens during the blocking process reflecting an increase of spatial correlations. We address the reliability of our predictions upon increasing the disorder or decreasing the fraction of processed structural information.

I. INTRODUCTION

Spatial networks represent systems in which the interconnected structure is embedded in real space. Examples range from transportation networks, power grids, and pedestrian crowds to granular materials and porous structures [1]. Spreading and transport processes on spatial networks have attracted much attention from both scientific and technological points of view [2–15]. Particularly, material transport through porous structures has been one of the basic problems of statistical physics [16, 17]. Despite the simple topology of spatial networks (compared to complex networks), transport on such structures exhibits an intriguing complexity due to the relevance of spatial dimensions, correlations and constraints, and dynamical evolution of structures. Achieving an optimal transport through a given spatial network requires a computationally costly analysis of structural information. Despite efforts (such as multiscale network analysis approach [18]), it is still an open challenge to reduce the huge computational costs by, for example, resorting to a partial information processing or taking advantage of structural self-similarities.

Optimal path models [19–25]— which minimize a cost function along possible routes in a disordered cost landscape— have been broadly employed in technological applications, e.g. internet routing and urban traffic, or to mimic natural processes such as transport in porous media, fracturing of heterogeneous materials, or electrical current through random structures [12, 26–33]. The drawback of frequently adopting optimal paths is the increased probability of their failure by congestion, overload, etc. To explore the resilience of spatial networks, the optimal path crack (OPC) model was introduced [20–22] in which the site with the highest cost along the optimal path is blocked, the next emerging optimal path is identified, and this procedure is repeated until the entire network is disconnected. The roughness of the resulting backbone, i.e. the disconnecting path, has been found to lie in the same universality class for various physical pro-

cesses with a fractal dimension of $d_f \simeq 1.2$ and 2.5 in two and three dimensions, respectively [20–22, 26, 34].

While the OPC model is based on processing the single optimal path information, past studies have shown that the relevance of network nodes for transport efficiency is better reflected in their betweenness centrality (BC) measure [35–38], defined as the total number of passing through a node when the entire set of optimal paths between all possible source-sink pairs is considered. Optimization of transport by prioritizing the flow through nodes with a higher BC is accompanied by an enhanced vulnerability of the system to the cascading failure of transport hubs subject to stochastic blockage events or targeted attacks [39–42]. It is expected that spatial networks display a higher degree of tolerance compared to, e.g., scale-free networks due to the possibility of nearly redundant routing between nodes. However, it is unclear how far a spatial network can adapt to successive blockage of transport hubs and what role the initial structure plays in approaching the onset of impenetrability.

Here we investigate the resilience of evolving spatial networks to effectively targeting the central transport hubs. By identifying the main hub in a porous lattice structure based on the BC measure of the nodes (see Fig. 1), we recursively block the hub and determine the next emerging one, until the system reaches the onset of impenetrability. We find a power-law scaling law for the required number of blocking steps with an exponent $d_f \simeq 1.05$ which is outside the statistical error bar of the OPC universality class exponent. Our results reveal a universal dependence of the number of blocking steps on the initial occupation fraction of the network, which enables us to predict the behavior for arbitrary large networks and different initial network densities. Besides benefiting from the predictive power of our discovery of structural self-similarities, the computational costs can be further reduced since we show that our predictions are remarkably robust against partial structural information processing. Following the evolution of the shortest-path length statistics reveals a gradual crossover from random

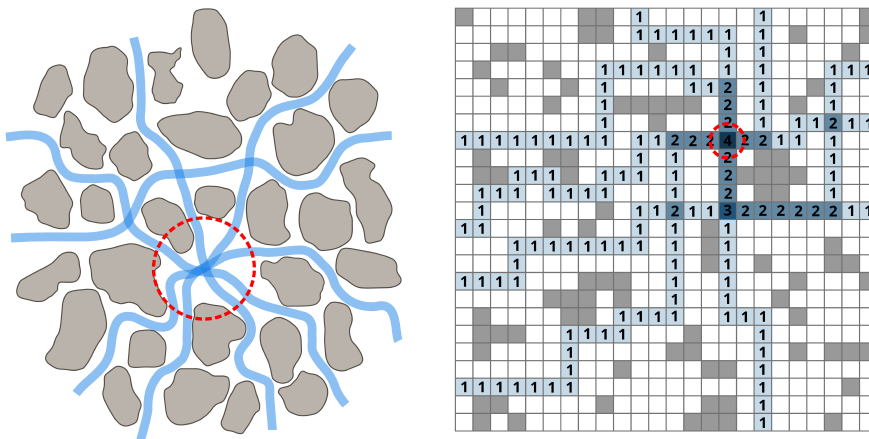


FIG. 1: (left) Schematic drawing of a porous medium. (right) Example of our porous lattice structures. A few optimal paths are shown in blue and the central transport hub is marked in red. The numbers in the right panel denote the non-zero centrality measures $\lambda(i, j)$ of the sites, defined in Eq. (1).

to correlated processes due to spatial exclusion effects.

II. POROUS LATTICE NETWORK MODEL

We consider a square lattice with S sites and reflective boundary conditions in all directions. An initial fraction ϕ_0 of the sites are randomly occupied in such a way that the structure remains connected. The main transport hub of the network is determined by evaluating the optimal paths between every possible pair of the lattice sites, using the Dijkstra shortest-path algorithm [43]. To avoid redundant shortest paths for each source-sink pair, a small random cost c_{ij} ($\ll 1/S$) is assigned to each empty site (i, j) while $c_{ij} = 1$ for occupied sites. The shortest path between two nodes is the one among all possible paths that has the smallest sum over all c_{ij} costs of its sites. Next, we assign a centrality measure $\lambda(i, j)$ to each site, defined as

$$\lambda(i, j) = \sum_{k \neq l} \sigma_{kl}(i, j), \quad (1)$$

where (k, l) indices run over all possible source-sink pairs. $\sigma_{kl}(i, j)$ is 1 if the shortest path between k and l nodes passes through the (i, j) site and 0 otherwise. The site with the highest λ is identified as the main transport hub and turned into an occupied site by changing its c_{ij} to 1. This procedure is then repeated until the network is disconnected. We define penetrability as having access from any existing source to any existing sink in the system. The blocking step at which this condition is violated is considered as the *onset of impenetrability* in our simulations. The network is disconnected beyond the onset of impenetrability, meaning that there is at least one isolated source or sink in the system. We denote the total number of blocked sites until reaching the onset of impenetrability with N_t and the length of the fault backbone (i.e. the line effectively breaking the network in two) with N_b . Although the exact computation of the centrality is extremely costly [18], for the simulation results presented in this manuscript we have exhaustively determined the

shortest path between all source-sink pairs (unless stated otherwise) to accurately identify the betweenness centrality measure for all nodes. Thus, the search for optimal path is repeated for $\mathcal{O}(S^2)$ pairs (i.e. linear lattice size to power four).

III. RESULTS

A. Structural self-similarities

We first consider a general case of an isotropic medium without a preferred flow direction and suppose that every pair of nodes across the entire network can be a possible source-sink transport set. Starting with an empty lattice ($\phi_0 = 0$), the number of blocking steps to reach the disconnection point is shown in Fig. 2(a) for different network sizes. Interestingly, N_t scales as $N_t \simeq S^{\beta/2}$ with an exponent $\beta = 1.61 \pm 0.01$. In contrast to the fault backbone in the OPC models, here the backbone does not necessarily pass across the network; the isotropicity of the endpoint positions of optimal paths enhances the transport through the bulk, favoring the formation of looped backbones in the central regions [see inset of Fig. 2(a)].

By exclusively choosing the source-sink pairs on the lattice boundaries, material fluxes through the bulk of the system reduce. This suggests that the blocked sites are distributed more uniformly across the network in this case, which enhances the probability of loopless backbone formation and increases the total number of required blocking steps to disconnect the network. The results shown in Fig. 2(a) confirm this hypothesis: N_t is larger for source-sink pairs on the boundaries compared to being across the entire network (similarly for the backbone length N_b ; not shown). Also the fractal dimension slightly increases to $\beta = 1.71 \pm 0.03$. In the lower inset of Fig. 2(a), a comparison is made to the inefficient strategy of randomly blocking the lattice sites; the inefficiency of this approach in disconnecting the structure slightly grows with increasing number of network nodes.

To clarify whether the fractal dimension of the backbone based on our BC measure lies in the OPC univer-

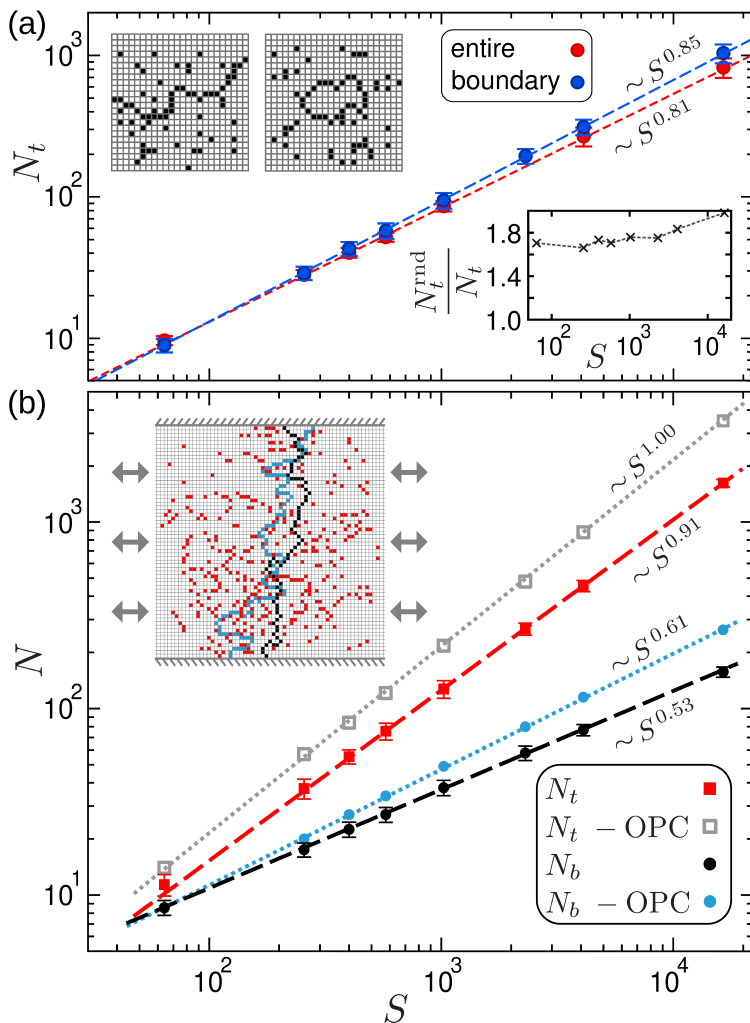


FIG. 2: (a) Total number of blocked sites N_t vs the number of network nodes S for $\phi_0=0$ and source-sink pairs being on the boundaries (blue circles) or across the entire network (red circles). The lines are power-law fits to the data. Insets: (top) Examples of disconnected networks with loopless or looped backbones. (bottom) Ratio of N_t for random and hierarchical site blockage versus S . (b) N_t and backbone length N_b vs S for source-sink pairs being on the vertical boundaries. A comparison is made to the OPC model results. Inset: Typical realization of the network at the onset of impenetrability. The backbone, other blocked sites, and an example of the OPC backbone are shown in black, red, and blue respectively.

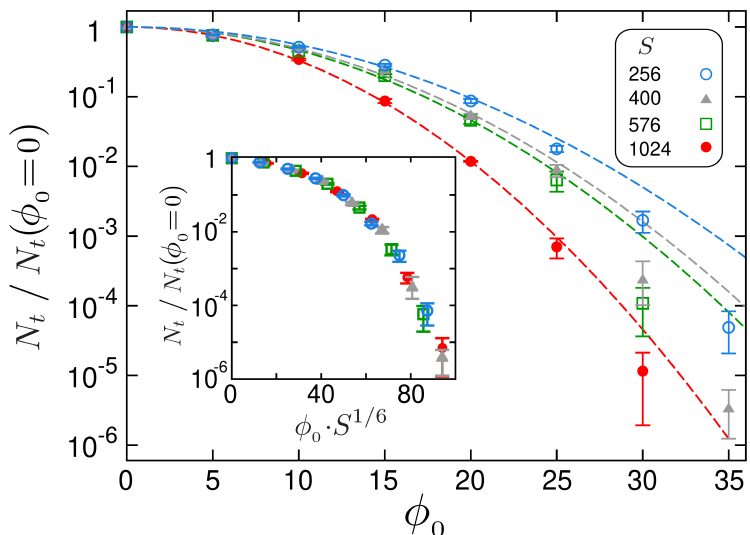


FIG. 3: Rescaled N_t versus the initial occupation fraction ϕ_0 for different network sizes. The dashed lines represent overall Gaussian fits to the data. Inset: Data collapse of the number of blocking steps versus the rescaled initial occupation fraction for different network sizes.

sality class, we further limit the choices of source-sink pairs to the vertical boundaries as in the OPC models; see inset of Fig. 2(b). Such an asymmetric transport eliminates the chance of looped backbone formation, resulting in larger N_t and N_b values than those for the

previously discussed symmetric conditions. Figure 2(b) reveals that our BC-based blockage brings the network to the impenetrability limit with a remarkably less number of blocking steps N_t and a lower power-law exponent ($\beta = 1.82 \pm 0.01$ vs 2.00 ± 0.01) compared to the OPC

model. Moreover, our backbones are visibly smoother than the OPC ones (see inset). The backbone length scales in both cases as $N_b \simeq S^{\gamma/2}$ but with a distinctly lower exponent $\gamma = 1.06 \pm 0.01$ in our simulations compared to 1.22 ± 0.02 in the OPC models [20–22, 26, 34], demonstrating that the backbone roughnesses of the two models belong to different universality classes.

Next, we address the role of the initial occupation fraction ϕ_0 of the structure (i.e. starting with $N_0 = \phi_0 S$ randomly occupied sites) in approaching the impenetrability limit. Here we show the results for source-sink pairs being across the entire network, but similar conclusions can be drawn for other boundary conditions. For a purely random blockage process, the average number of blocking steps to disconnect the structure follows $N_t(\phi_0) = N_t(\phi_0=0) - \phi_0 S$, imposing an upper limit $\phi_0^{\max} = N_t(\phi_0=0)/S$ for the initial occupation fraction of the network to remain connected. However, we can increase ϕ_0 beyond ϕ_0^{\max} by selecting only the connected initial structures. The BC-based hierarchical site elimination procedure is then applied to disconnect these structures. Figure 3 displays a network size-dependent decay of N_t versus ϕ_0 , with a faster than a Gaussian tail (which can be roughly captured by a Cauchy distribution, probably reflecting the heterogeneity of the initial sampling). At a given ϕ_0 , the deviations grow with decreasing S , along with the increasing difficulty in finding connected initial structures. Importantly, the data collapses onto a single master curve for different S when ϕ_0 axis is rescaled by $S^{1/6}$; see inset of Fig. 3. This implies that the number of steps to block a network with a given initial occupation fraction ϕ_0 scales as

$$N_t(\phi_0) = S^{\beta/2} \tilde{N}_t(\phi_0 \cdot S^{1/6}), \quad (2)$$

with $\tilde{N}_t(0) = 1$.

B. Evolution of spatial correlations

Past studies attempted to evaluate the BC distribution on various static spatial networks [38, 44], suggesting, e.g., a fast BC decay of the form $1 - r^2/S$ (r being the distance from the network center) in highly porous structures. However, it is unclear how the spatial distribution of centralities evolves during a cascading failure of high BC nodes under a targeted attack. By measuring the blocking probability $p(r)$ in our dynamically evolving porous lattice structures, we find that the behavior is well captured by a Gaussian radial decay

$$p(r) \sim \exp\left[-\frac{1}{2}\left(\frac{r}{\sqrt{S}/2}\right)^2\right] \quad (3)$$

for source-sink pairs being across the entire network. Choosing the pairs on the boundaries diminishes the importance of the central regions, leading to a plateau at small r ; nevertheless, the tail of $p(r)$ towards the corners

still satisfactorily follows Eq.(3); see Fig.4 and insets. As a result of the rapid radial decay of the importance of sites for homogeneously distributed sources and sinks, blockage of the transport hubs mostly occurs in the central region which leads to looped backbone formation. By distributing the sources and sinks on the boundaries, the shortest paths do not necessarily pass through the center of the system and the importance of the sites becomes spatially more uniform, which promotes loopless backbones. To better understand the morphological transition from looped to loopless backbones (e.g. to clarify whether it is a continuous or discontinuous transition), the sinks and sources can be gradually pushed away from the center of the network [45]. However, such a study is computationally costly and beyond the scope of the present work. A similar morphological transition has been reported in the context of optimal transportation networks [46]. Compared to static spatial networks, the slower decay of $p(r)$ in our evolving structures in the course of blocking process indicates growing spatial correlations and constraints. A higher chance of site elimination in central regions creates bottlenecks and, thus, new high BC sites in these regions. This process self-amplifies and leads to a slower spreading of the emerging transport hubs across the network. Formation of bottlenecks in the bulk causes longer shortest-paths ℓ , affecting the shortest-path length statistics. The shortest-path length distribution $f(\ell)$ is shown in Fig.5 at different stages n of the blocking process. It can be seen that $f(\ell)$ broadens during the blocking process with a tail gradually evolving from a Gaussian towards a gamma distribution $\frac{\ell^{\sigma-1}}{\lambda^\sigma \Gamma(\sigma)} \exp(-\ell/\lambda)$ associated with random events in the presence of self-correlations [47–49] (see inset). $f(\ell)$ eventually develops a bimodal shape at the latest blocking stages before the onset of impenetrability because the network practically splits into two islands whose connection through the remaining bottlenecks creates the secondary peak of $f(\ell)$ at longer shortest-paths.

C. Robustness of results

Finally, we address the stability of our findings against incomplete structural information. This includes uncertainty in the initial cost landscape and/or a partial processing of the structural information. We first modify the initial conditions by changing the random cost c_{ij} of each empty site (i, j) within a uniform variation range around the original value. Starting from this new cost landscape, we obtain the number of blocking steps and the backbone path and compare them with those of the original cost landscape. N_t does not show systematic dependence on the variations (or inaccuracies in the measurements) of the cost landscape (not shown), indicating that our prediction of transport resilience and onset of impenetrability is reliable. However, the results shown in the inset of Fig.6 demonstrate that the backbone path

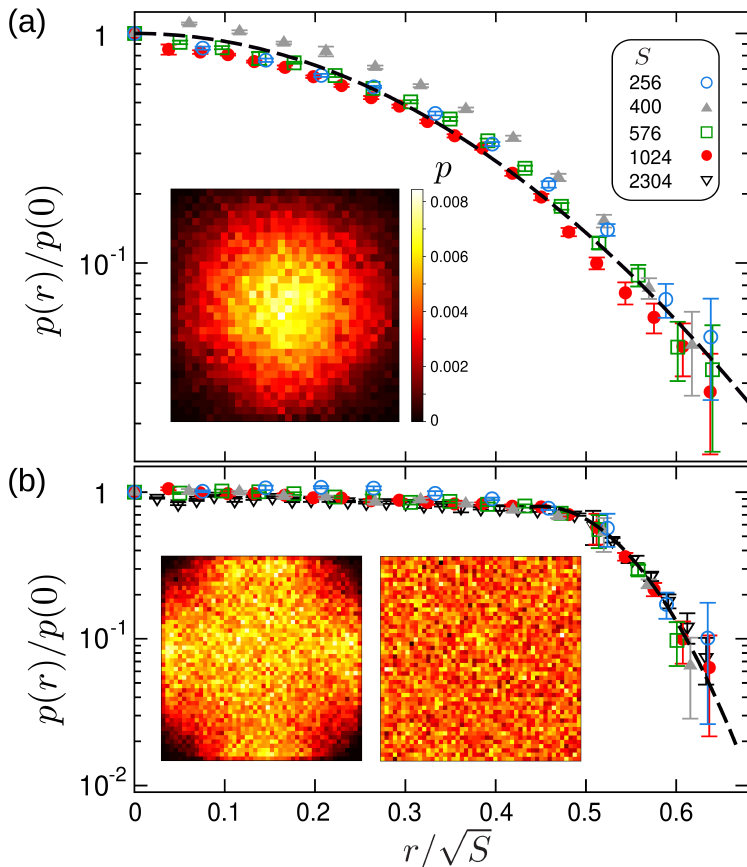


FIG. 4: Blocking probability $p(r)$ of sites versus their radial distance r from the center of the structure for different network sizes and source-sink pairs being (a) across the entire network or (b) on the boundaries. The dashed lines show a Gaussian fit, Eq. (3). The insets show the spatial distribution of $p(r)$ (The right inset of panel (b) represents a random blockage process for comparison).

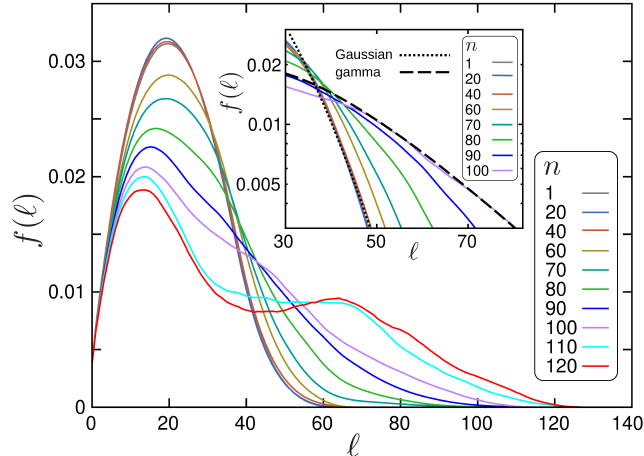


FIG. 5: Probability distribution of the shortest-path length ℓ at different stages n of the blocking process. The inset zooms in on the tail behavior. The dotted and dashed lines indicate Gaussian and gamma distributions as a guide to the eye.

is highly sensitive to the cost landscape variations; even 1% change of c_{ij} values results in a new backbone with less than 25% overlap with the original backbone. Thus, a precise knowledge of the cost landscape is crucial for predicting the exact backbone path in porous lattice net-

works. Figure 6 also reveals that the results are highly robust against an incomplete processing of the structural information, i.e., if only a fraction of the source-sink pairs are randomly chosen to evaluate the centrality measures $\lambda(i, j)$ at each blocking step. We vary the fraction of processed source-sink pairs for a network with $S = 4096$ nodes from 100% ($\sim 10^7$ pairs) to 10% ($\sim 10^6$ randomly chosen pairs) to assess the robustness of the results. It can be seen that by processing of only 25% of all possible routes, the change in the number of blocking steps still remains below 5%. This promises the possibility of significant reduction of computational costs in the BC-based evaluation of main transport hubs according to our proposed approach.

IV. CONCLUSION

In conclusion, we have shown that the optimization of transport through evolving porous lattice structures based on the centrality measure of the nodes has the drawback of reduced adaptability and resilience of the spatial network during a cascading failure of main transport hubs subject to stochastic blockage events or targeted attacks. Our findings of universal resilience of spatial networks allow for predicting the number of blocking steps to reach the onset of impenetrability for different network sizes and occupation densities. Trans-

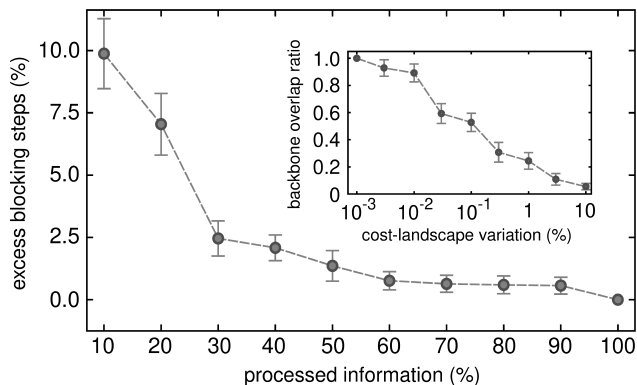


FIG. 6: Excess number of required blocking steps in terms of the fraction of randomly processed source-sink pairs to evaluate the centrality measures $\lambda(i, j)$ at each blocking step, for pairs being across the entire network with $S = 4096$ nodes. Inset: Deviation of the backbone path from the original one upon increasing the variation range of the random costs c_{ij} of empty sites around their original values.

port on dynamic porous lattice structures is typical of many problems in this class. We expect that our findings and conclusions hold for a broad range of real-world spatial networks and welcome work in this area. The reliability of our predictions upon considerable reduction of the amount of structural information processing can be combined with multiscale analysis approaches to further reduce the computational costs, which is crucial for practical and technological applications. The differences between the universality class of centrality-based node elimination and the OPC models deserve to be further studied on other topologies in spatial networks and for correlated cost landscapes. These remain exciting open challenges toward better understanding and designing of transport processes under disturbances and to improve the adaptation and recovery of transport capacity in dynamically evolving structures.

Acknowledgments

This work was supported by the Deutsche Forschungsgemeinschaft (DFG) via grants INST 256/539-1, which funded the computing resources at Saarland University.

-
- [1] Barthélemy, M. Spatial networks. *Phys. Rep.* **499**, 1–101 (2011).
- [2] Çolak, S., Lima, A. & González, M. C. Understanding congested travel in urban areas. *Nat. Commun.* **7**, 10793 (2016).
- [3] Ren, Y., Ercsey-Ravasz, M., Wang, P., González, M. C. & Toroczkai, Z. Predicting commuter flows in spatial networks using a radiation model based on temporal ranges. *Nat. Commun.* **5**, 5347 (2014).
- [4] Morris, R. G. & Barthelemy, M. Transport on coupled spatial networks. *Phys. Rev. Lett.* **109**, 128703 (2012).
- [5] González, M. C., Hidalgo, C. A. & Barabási, A.-L. Understanding individual human mobility patterns. *Nature* **453**, 779–782 (2008).
- [6] Shaebani, M. R., Sadjadi, Z., Sokolov, I. M., Rieger, H. & Santen, L. Anomalous diffusion of self-propelled particles in directed random environments. *Phys. Rev. E* **90**, 030701 (2014).
- [7] Kartun-Giles, A. P., Barthelemy, M. & Dettmann, C. P. Shape of shortest paths in random spatial networks. *Phys. Rev. E* **100**, 032315 (2019).
- [8] Kang, P. K., Dentz, M., Le Borgne, T. & Juanes, R. Spatial markov model of anomalous transport through random lattice networks. *Phys. Rev. Lett.* **107**, 180602 (2011).
- [9] Zhang, L. *et al.* Scale-free resilience of real traffic jams. *Proc. Natl. Acad. Sci. U.S.A.* **116**, 8673–8678 (2019).
- [10] Li, D. *et al.* Percolation transition in dynamical traffic network with evolving critical bottlenecks. *Proc. Natl. Acad. Sci. U.S.A.* **112**, 669–672 (2015).
- [11] Shaebani, M. R., Jose, R., Sand, C. & Santen, L. Unraveling the structure of treelike networks from first-passage times of lazy random walkers. *Phys. Rev. E* **98**, 042315 (2018).
- [12] Carmona, H. A., de Noronha, A. W. T., Moreira, A. A., Araújo, N. A. M. & Andrade, J. S. Cracking urban mobility. *Phys. Rev. Res.* **2**, 043132 (2020).
- [13] Zeng, G. *et al.* Switch between critical percolation modes in city traffic dynamics. *Proc. Natl. Acad. Sci. U.S.A.* **116**, 23–28 (2019).
- [14] Olmos, L. E., Colak, S., Shafiei, S., Saberi, M. & Gonzalez, M. C. Macroscopic dynamics and the collapse of urban traffic. *Proc. Natl. Acad. Sci. U.S.A.* **115**, 12654–12661 (2018).
- [15] Fouladvand, M. E., Sadjadi, Z. & Shaebani, M. R. Optimized traffic flow at a single intersection: traffic responsive signalization. *J. Phys. A* **37**, 561 (2004).
- [16] Hunt, A. G. & Sahimi, M. Flow, transport, and reaction in porous media: Percolation scaling, critical-path analysis, and effective medium approximation. *Rev. Geophys.* **55**, 993–1078 (2017).
- [17] Meakin, P. & Tartakovsky, A. M. Modeling and simulation of pore-scale multiphase fluid flow and reactive transport in fractured and porous media. *Rev. Geophys.* **47**, RG3002 (2009).
- [18] Ercsey-Ravasz, M. & Toroczkai, Z. Centrality scaling in large networks. *Phys. Rev. Lett.* **105**, 038701 (2010).
- [19] Hansen, A. & Kertész, J. Phase diagram of optimal paths. *Phys. Rev. Lett.* **93**, 040601 (2004).
- [20] Andrade, J. S., Oliveira, E. A., Moreira, A. A. & Herrmann, H. J. Fracturing the optimal paths. *Phys. Rev. Lett.* **103**, 225503 (2009).
- [21] Oliveira, E. A., Schrenk, K. J., Araújo, N. A. M., Herrmann, H. J. & Andrade, J. S. Optimal-path cracks in correlated and uncorrelated lattices. *Phys. Rev. E* **83**, 046113 (2011).
- [22] Fehr, E. *et al.* Corrections to scaling for watersheds, optimal path cracks, and bridge lines. *Phys. Rev. E* **86**,

- 011117 (2012).
- [23] Sampaio Filho, C. I. N., Andrade, J. S., Herrmann, H. J. & Moreira, A. A. Elastic backbone defines a new transition in the percolation model. *Phys. Rev. Lett.* **120**, 175701 (2018).
- [24] Talon, L., Auradou, H., Pessel, M. & Hansen, A. Geometry of optimal path hierarchies. *Europhys. Lett.* **103**, 30003 (2013).
- [25] Folz, F., Mehlhorn, K. & Morigi, G. Noise-induced network topologies. *Phys. Rev. Lett.* **130**, 267401 (2023).
- [26] Moreira, A. A. *et al.* Fracturing highly disordered materials. *Phys. Rev. Lett.* **109**, 255701 (2012).
- [27] Schrenk, K. J., Araújo, N. A. M., Andrade Jr, J. S. & Herrmann, H. J. Fracturing ranked surfaces. *Sci. Rep.* **2**, 348 (2012).
- [28] Sharafedini, E., Hamzhepour, H. & Alidoust, M. Statistical quantum conductance of porous and random alloys. *Appl. Phys. Lett.* **123**, 172104 (2023).
- [29] Hamzhepour, H., Atakhani, A., Gupta, A. K. & Sahimi, M. Electro-osmotic flow in disordered porous and fractured media. *Phys. Rev. E* **89**, 033007 (2014).
- [30] Fehr, E., Kadau, D., Andrade, J. S. & Herrmann, H. J. Impact of perturbations on watersheds. *Phys. Rev. Lett.* **106**, 048501 (2011).
- [31] Sharafedini, E., Hamzhepour, H., Masoudi, S. F. & Sahimi, M. Electrical conductivity of the films grown by ballistic deposition of rodlike particles. *J. Appl. Phys.* **118**, 215302 (2015).
- [32] Oliveira, E. A. *et al.* A universal approach for drainage basins. *Sci. Rep.* **9**, 9845 (2019).
- [33] Hamzhepour, H., Kasani, F. H., Sahimi, M. & Sepehrinia, R. Wave propagation in disordered fractured porous media. *Phys. Rev. E* **89**, 023301 (2014).
- [34] Daryaei, E., Araújo, N. A. M., Schrenk, K. J., Rouhani, S. & Herrmann, H. J. Watersheds are schramm-loewner evolution curves. *Phys. Rev. Lett.* **109**, 218701 (2012).
- [35] Newman, M. E. J. Scientific collaboration networks. ii. shortest paths, weighted networks, and centrality. *Phys. Rev. E* **64**, 016132 (2001).
- [36] Noh, J. D. & Rieger, H. Random walks on complex networks. *Phys. Rev. Lett.* **92**, 118701 (2004).
- [37] Goh, K.-I., Kahng, B. & Kim, D. Universal behavior of load distribution in scale-free networks. *Phys. Rev. Lett.* **87**, 278701 (2001).
- [38] Kirkley, A., Barbosa, H., Barthelemy, M. & Ghoshal, G. From the betweenness centrality in street networks to structural invariants in random planar graphs. *Nat. Commun.* **9**, 2501 (2018).
- [39] Albert, R., Jeong, H. & Barabási, A.-L. Error and attack tolerance of complex networks. *Nature* **406**, 378–382 (2000).
- [40] Holme, P., Kim, B. J., Yoon, C. N. & Han, S. K. Attack vulnerability of complex networks. *Phys. Rev. E* **65**, 056109 (2002).
- [41] Bashan, A., Berezin, Y., Buldyrev, S. V. & Havlin, S. The extreme vulnerability of interdependent spatially embedded networks. *Nat. Phys.* **9**, 667–672 (2013).
- [42] Buldyrev, S. V., Parshani, R., Paul, G., Stanley, H. E. & Havlin, S. Catastrophic cascade of failures in interdependent networks. *Nature* **464**, 1025–1028 (2010).
- [43] Dijkstra, E. W. A note on two problems in connexion with graphs. *Numer. Math.* **1**, 269–271 (1959).
- [44] Verbavatz, V. & Barthelemy, M. Betweenness centrality in dense spatial networks. *Phys. Rev. E* **105**, 054303 (2022).
- [45] We thank an anonymous referee for the valuable suggestion.
- [46] Aldous, D. & Barthelemy, M. Optimal geometry of transportation networks. *Phys. Rev. E* **99**, 052303 (2019).
- [47] Vliгентhart, G. A. & Gompfer, G. Forced crumpling of self-avoiding elastic sheets. *Nat. Mater.* **5**, 216–221 (2006).
- [48] Shaebani, M. R., Najafi, J., Farnudi, A., Bonn, D. & Habibi, M. Compaction of quasi-one-dimensional elastoplastic materials. *Nat. Commun.* **8**, 15568 (2017).
- [49] Deboeuf, S., Katzav, E., Boudaoud, A., Bonn, D. & Adda-Bedia, M. Comparative study of crumpling and folding of thin sheets. *Phys. Rev. Lett.* **110**, 104301 (2013).